

Effects of a staircase on minigaps in Si inversion layers

Fusayoshi J. Ohkawa*

Department of Physics, University of California, San Diego, La Jolla, California 92093

(Received 23 January 1981)

Effects of one-dimensional periodic staircases on minigaps are theoretically investigated. Various cases are classified according to the step height. Observed positions of minigaps can be explained by a staircase model whose step height is half a lattice constant. In this case (i) the minigaps are assigned from the lowest as $E_0, E_1, A_1, E_{-1}, E_2, A_2, E_{-2}$, and so on, where E stands for an intervalley minigap and A for an intravalley one; (ii) E , observed in dc conduction are approximately given by $E_r \approx 23(\theta/\alpha) \exp[-(1/4)r^2 W^2] \sin(2\phi) N_{\text{eff}}$ (meV) for $|r|\pi\alpha\theta < 1$, where θ and ϕ are polar and azimuthal angles of tilting, α is a parameter expressing a step structure and of the order of one, W is a parameter specifying the disorder of staircase, and $N_{\text{eff}} = (N_{\text{inv}} + 3N_{\text{dep}})/10^{12}$ cm $^{-2}$; (iii) $A_r \approx [(0.46/r)^2 + 83^2(\theta/\alpha - 2\theta^2)^2 N_{\text{eff}}^{-2/3}]^{1/2} \exp[-(1/4)r^2 W^2] N_{\text{eff}}$ (meV); (iv) uniaxial stress along $[110]$ or $[1\bar{1}0]$ has an effect on E_r .

I. INTRODUCTION

Minigaps in Si inversion layers slightly tilted from the (001) plane have been extensively studied both experimentally and theoretically for the past years.¹ Anomalous structures caused by minigaps are observed in several measurements such as dc conduction in the absence of magnetic fields,^{2,3} Shubnikov-de Haas oscillations,^{4,5} optical resonance,⁶⁻¹² and photoconductivity measurements.^{12,13}

A conduction band of Si has six valley minima along Δ axes near X points. The two valleys along the $[001]$ axis give rise to the ground subbands in vicinal planes of (001). Therefore, there are two kinds of minigaps: intravalley ones and intervalley ones. Cole, Lakhani, and Stiles² proposed a mechanism whereby minigaps are opened by one-dimensional superlattices, or staircase structures. Since their original model considers only intravalley minigaps, it is very difficult to explain the position of the lowest minigaps in terms of a periodicity of staircases.

Sham, Allen, Kamgar, and Tsui⁶ proposed an alternative explanation called a valley projection model, which can explain the observed positions of the minigaps. They constructed a two-dimensional Brillouin zone by projecting a three-dimensional one, and claim that minigaps are formed at crossing points in such a two-dimensional band structure. Their model includes intervalley minigaps as well as intravalley ones.

Sham¹⁵ investigated the valley projection model more precisely. Volkov and Sandomirskii¹⁴ also investigated a staircase model which includes intervalley minigaps as well as intravalley ones. These two models are exactly the same as far as the positions of minigaps are concerned. The valley projection model by Sham, Allen, Kamgar, and Tsui is the simplest version of the general one. On the basis of this result, Volkov and Sandomirskii claimed that the minigaps,

other than those predicted by the simplest model, should be observed in certain planes such as (2223). However, the current experimental results seem to show that the minigaps predicted only by the general model are too small to be observed.³

The positions of the minigaps can be obtained by a geometrical discussion in the valley projection model and/or the staircase model. If the staircase model is taken, the periodicity should be $a/(2 \sin\theta)$ to explain the experiments; a is the lattice constant of Si ($a = 5.43 \text{ \AA}$). The theoretical estimates for the magnitudes of minigaps have been made so far in flat interfaces.¹⁵⁻¹⁸ Although the lowest minigap can be partly explained by these theories,¹⁸ the higher minigaps cannot be explained.

In the present paper, we study the effects of periodic staircases on the minigaps. Since we have at present some information about staircases constructed on MOS (metal-oxide-semiconductor) interfaces tilted slightly from (001),^{19,20} it is of interest to make models and to compare the theoretical results obtained in these models to the experimental results. We can determine by that procedure what actual interfaces look like. This is the aim of the present paper, although enough experimental data are not available in the present stage. A Hamiltonian is presented in Sec. II. The Hamiltonian includes only the so-called X -point coupling. Various staircase models are discussed in Sec. III. The magnitudes of the minigaps are evaluated in Sec. IV on the basis of the staircase models discussed in Sec. III. Discussion is presented in Sec. V, and the results are summarized in Sec. VI.

II. HAMILTONIAN

First, we define a coordinate system used here. Let us consider the (lmn) plane, where n is much larger than l and m . Crystal axes $[100]$,

[010], and [001] are denoted by x , y , and z axes, respectively. The axis $[lmn]$ is normal to the interface, and is defined as the ζ axis. The other two axes $[lnmn - l^2 - m^2]$, and $[-ml\ 0]$ are parallel to the interface, and are denoted by the ξ and η axes, respectively. Tilting of the (lmn) plane

from (001) is expressed in terms of a polar angle $\theta = \cos^{-1}[n/(l^2 + m^2 + n^2)^{1/2}]$ and an azimuthal one $\phi = \cos^{-1}[l/(l^2 + m^2)^{1/2}]$.

Our starting Hamiltonian is an X -point $\vec{k} \cdot \vec{p}$ Hamiltonian obtained by Hensel, Hasegawa, and Nakayama,²¹

$$\mathcal{H} = \begin{bmatrix} \frac{\hbar^2}{2m_t} (k_x^2 + k_y^2) + \frac{\hbar^2}{2m_l} (k_z + K)^2 & \frac{\hbar^2}{2m} L k_x k_y + \Xi e_{xy} \\ \frac{\hbar^2}{2m} L k_x k_y + \Xi e_{xy} & \frac{\hbar^2}{2m_t} (k_x^2 + k_y^2) + \frac{\hbar^2}{2m_l} (k_z - K)^2 \end{bmatrix} + V(\xi), \quad (1)$$

where k_z is measured from the X point, and $K = 0.15(2\pi/a)$: wave vectors k_α are to be interpreted as operators ($-i\partial/\partial x_\alpha$); $m_t = 0.1905 m$, $m_l = 0.9163 m$, $L \geq 8.53$, e_{xy} is a shear strain component, and Ξ is its deformation potential; $V(\xi)$ is an inversion layer potential. This Hamiltonian includes only the X -point inter-valley coupling. In an exact (001) plane, the Γ -point coupling plays a major role as discussed by Ohkawa and Uemura,²² and Sham and Nakayama.²³ However, it plays a minor role in tilted planes. It is assumed in the present investigation that a polar angle θ of tilting is much less than one in radians, but not so small that the X coupling might be a major contribution.

The boundary condition is that wave functions vanish at the interface $\zeta = \Delta(\xi, \eta)$. Because this boundary condition is very difficult to treat, we take the following unitary transformation similar to that used in the treatment of the surface roughness scatterings,²⁴

$$U = \begin{bmatrix} \exp\left(\Delta(\xi, \eta) \frac{\partial}{\partial \xi}\right) \exp(iK \cos \theta \xi) & 0 \\ 0 & \exp\left(\Delta(\xi, \eta) \frac{\partial}{\partial \xi}\right) \exp(-iK \cos \theta \xi) \end{bmatrix}, \quad (2)$$

which is a product of a translation in the momentum space and a translation in the real space. The Hamiltonian to be solved is UHU^{-1} . Because of a translation in the real space, the boundary condition turns out to be very simple; wave functions should vanish at $\zeta = 0$.

When the effects of higher subbands are neglected, the Hamiltonian becomes much simpler,

$$\begin{aligned} \mathcal{H}_1 &= PUHU^{-1}P^{-1} \\ &= \begin{bmatrix} h_{11} & h_{12} \\ h_{12}^* & h_{22} \end{bmatrix}, \end{aligned} \quad (3)$$

where P is a projection operator to the Hilbert space of the ground subbands,

$$h_{11} = \frac{\hbar^2}{2m_t} [(k_t - \theta K)^2 + k_\eta^2] + F\Delta + T \left[\left(\frac{\partial \Delta}{\partial \xi} \right)^2 + \left(\frac{\partial \Delta}{\partial \eta} \right)^2 \right], \quad (4)$$

$$h_{22} = \frac{\hbar^2}{2m_t} [(k_t + \theta K)^2 + k_\eta^2] + F\Delta + T \left[\left(\frac{\partial \Delta}{\partial \xi} \right)^2 + \left(\frac{\partial \Delta}{\partial \eta} \right)^2 \right], \quad (5)$$

and

$$\begin{aligned} h_{12} &= \Xi e_{xy} e^{i2K\Delta} S_0 + \frac{\hbar^2 L}{2m} e^{iK\Delta} \left\{ \frac{1}{2} \sin 2\phi \left[(k_t^2 - k_\eta^2) S_0 + \left(\theta - \frac{\partial \Delta}{\partial \xi} \right)^2 S_2 - \left(\frac{\partial \Delta}{\partial \eta} \right)^2 S_2 \right] \right. \\ &\quad \left. + \cos 2\phi \left[k_t k_\eta S_0 - \left(\theta - \frac{\partial \Delta}{\partial \xi} \right) \frac{\partial \Delta}{\partial \eta} S_2 \right] \right\} e^{iK\Delta}, \end{aligned} \quad (6)$$

with

$$F = \int_{+0}^{\infty} d\xi \frac{\partial V}{\partial \xi} \phi^2(\xi), \quad (7)$$

$$T = \frac{\hbar^2}{2m_t} \int_0^{\infty} d\xi \phi \left(-i \frac{\partial}{\partial \xi} \right)^2 \phi, \quad (8)$$

and

$$S_r = \int_0^{\infty} d\xi e^{ik_z \xi} \phi(\xi) \left(-i \frac{\partial}{\partial \xi} \right)^r e^{ik_z \xi} \phi(\xi). \quad (9)$$

Wave function $\phi(\xi)$ belongs to the ground subband, which satisfies the following Schrödinger equation:

$$\left[\frac{\hbar^2}{2m_t} \left(-i \frac{\partial}{\partial \xi} \right)^2 + V(\xi) \right] \phi(\xi) = \epsilon \phi(\xi). \quad (10)$$

In the present paper, a nearly self-consistent wave function ϕ is used.²² Here it should be noted that S_1 is identically zero.

Our Hamiltonian is of a 2×2 form. The first component, which expresses a valley in positive k_z , is defined as plus (+) valley, and the second component as minus (-) valley; we assume without loss of generality that θ is positive.

III. STAIRCASE MODEL

The staircase model by Volkov and Sandomirskii¹⁴ can predict the shortest possible periodicity that is commensurate to an Si lattice, and it is exactly the same as that predicted by the valley projection model by Sham.¹⁵ However, their staircase model still has an ambiguity about a step structure: How high are steps? What staircase structures are realized in actual samples depends on the sample preparation. Therefore, various possible cases are discussed in the present paper.

The shortest possible height of steps is a quarter-lattice constant ($a/4$), because a Si lattice is of a diamond type. Therefore, we assume tentatively that almost all steps are $ja/4$ where j is a non-negative integer; the case of $j=0$ means that an interface is flat. A periodicity in the real space is $(ja)/(4 \sin \theta)$. Because a periodicity should be commensurate to an Si lattice, as pointed out by Volkov and Sandomirskii, this model should be modified a little as discussed later.

Although there is a problem of whether staircase structures are one dimensional or two dimensional, we take a one-dimensional model for the sake

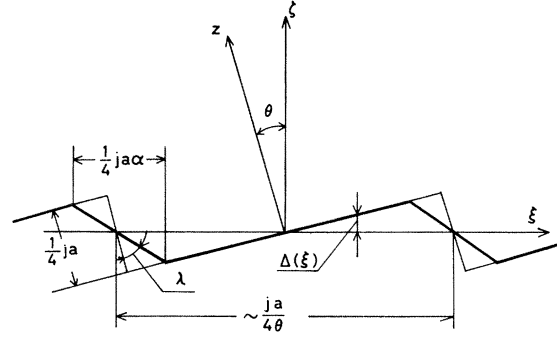


FIG. 1. A staircase model in (lmn) plane. Axis z is $[001]$ and ξ is $[lmn]$. Angle θ is a polar angle of tilting and a is the lattice constant of Si (5.43 Å).

of simplicity. The s th step is located in the neighborhood of $\xi_s = (sja)/(4 \sin \theta)$, because the interface should be macroscopically flat. The probability of finding the s th step at ξ is assumed to be

$$P_s(\xi) = \frac{1}{\sqrt{\pi} \Delta \xi} \exp \left(- \frac{(\xi - \xi_s)^2}{(\Delta \xi)^2} \right), \quad (11)$$

although the actual distribution should be a discrete one because of a lattice structure; this is the first approximation to include the disorder.

An interface location $[z = \Delta(\xi)]$ is a function of ξ and is defined as in Fig. 1. Because the step structure is not well known, our staircase model includes a parameter α or λ , which is shown in Fig. 1.

In the present paper, the randomness is treated by ensemble averages. For example, the following quantities are necessary in the present investigations;

$$\langle \Delta(\xi) \rangle = \sum_{r=-\infty}^{\infty} b_r \exp \left(i \frac{8r\pi\theta}{ja} \xi \right) \quad (12)$$

and

$$\left\langle \left(\mu = \frac{\partial \Delta}{\partial \xi} \right)^2 \right\rangle = \sum_{r=-\infty}^{\infty} C_r(\mu) \exp \left(i \frac{8r\pi\theta}{ja} \xi \right). \quad (13)$$

Here $\langle \rangle$ means the ensemble average,

$$b_r = -i(-1)^r \frac{ja}{8r\pi} \frac{\sin(r\pi\theta\alpha)}{r\pi\theta\alpha} e^{-(r/n)^2 w^2}, \quad (14)$$

and

$$C_r(\mu) = \begin{cases} \frac{\theta}{\alpha} + \mu^2 - \theta^2 & (r=0) \\ (-1)^r \frac{\theta}{\alpha} [1 + 2\alpha(\mu - \theta)] \frac{\sin(r\pi\theta\alpha)}{r\pi\theta\alpha} e^{-(r/n)^2 w^2} & (r \neq 0), \end{cases} \quad (15)$$

where $W = (4\pi\theta)\Delta\xi/a$ and $\alpha = \sin(\theta + \lambda)/\cos\lambda$.

Because a periodic staircase structure plays a role in the intervalley couplings as well as intravalley ones, a one-dimensional Brillouin zone as shown in Fig. 2 can be constructed. The size of the first mini-Brillouin zone is $2Q/j$ with $Q = 4\pi\theta/a$. There are two types of minigaps: intervalley minigaps and intravalley minigaps. Intervalley ones are denoted by E_r and intravalley ones by A_r , where r means that the r th Fourier component in Eq. (12) or (13) is responsible for E_r and A_r . In the extended-zone scheme, the valley minima are located at $k_x = \pm 0.15(Q/2)$, E_r at $k_x = \pm rQ/j$, and A_r at $k_x = \pm[(0.15/2) + (r/j)]Q$ and $\pm[(0.15/2) - (r/j)]Q$. Therefore, the lowest minigap is E_0 , as long as j is less than or equal to 6, i.e., as long as step heights are less than or equal to $(6/4)a$. Otherwise the lowest one is E_1 . When $j=0$, that is, when the interface is flat, only E_0 is finite in our Hamiltonian.

So far, we have assumed that a periodicity in the real space is commensurate to the lattice structure. However, it is not generally the case. For example, let us consider the (118) plane with step height $a/2$ ($j=2$). As the valley projection model, or Volkov and Sandomirskii's staircase model shows, a commensurate periodicity is not $a/(2\sin\theta)$, but $a/\sin\theta$. Therefore, the fundamental Fourier component of periodic staircases is $2\pi\sin\theta/a$. However, this component is very

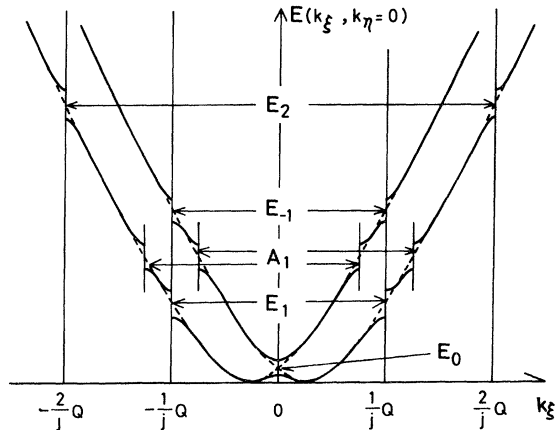


FIG. 2. Surface band structure in the extended-zone scheme. Because an X -point $\vec{k} \cdot \vec{p}$ Hamiltonian is used, the center of the mini-Brillouin zone corresponds to X . Intervalley minigaps are denoted by E_r ($-\infty < r < \infty$), and intravalley ones by A_r ($r \geq 1$). The size of the first mini-Brillouin zone is $(2/j)Q$ with $Q = 4\pi\theta/a$, when step heights are $ja/4$. In an incommensurate case, very small new minigaps are expected as well as those shown here.

small because of the following two reasons:

(i) As far as all the step heights are $a/2$, the $2\pi\sin\theta/a$ component is much smaller than the $4\pi\sin\theta/a$ component, and (ii) the disorder makes the $2\pi\sin\theta/a$ component much smaller than the $4\pi\sin\theta/a$ component. Very small minigaps can be expected at the positions predicted by the Fourier component $2\pi\sin\theta/a$. As far as the major minigaps are concerned, the commensurability of the period does not have to be taken into account.

So far it is assumed that almost all steps have the same height, that is $ja/4$. If various steps are mixed up, the sample can be regarded as one with the highest steps that are realized in a significant number, and with a lot of disorder.

IV. MINIGAPS

Intervalley minigaps open at $k_x = (r/j)Q$ with $Q = 4\pi\theta/a$, as shown in Fig. 2. In the present paper the first-order effects with respect to the off-diagonal term h_{12} are evaluated.

Because Δ is assumed not to depend on η , k_η in the Hamiltonian can be regarded as c numbers. The matrix element of h_{12} between $[k_x = (r/j)Q, +]$ and $[k_x = -(r/j)Q, -]$ has to be evaluated:

$$M_r = 2 \langle (r/j)Q | \langle h_{12} \rangle | -(r/j)Q \rangle \\ = \left(2\Xi e_{xy} + \frac{\hbar^2 L}{2m} k_\eta^2 \right) [\delta_{r0} + i2Kb_r(1 - \delta_{r0})] S_0 \\ + \frac{\hbar^2 L}{2m} \left[-S_0 K^2 C_r \left(\frac{rQ}{jK} \right) + S_2 C_r(\theta) \right], \quad (16)$$

where δ_{r0} is the Kronecker delta, b_r and C_r are defined in Eqs. (14) and (15). Use is made of a relation

$$\int d\xi e^{-irQ\xi/j + iK\Delta} k_x^2 e^{-irQ\xi/j + iK\Delta} \\ = -K^2 \int d\xi e^{-i2rQ\xi/j + i2K\Delta} \left(\frac{rQ}{jK} - \frac{\partial \Delta}{\partial \xi} \right)^2, \quad (17)$$

and of an approximation $\exp(i2K\Delta) \approx 1$ in evaluating the terms proportional to $(\mu - \partial\Delta/\partial\xi)^2$. Since $2K|\Delta|$ is less than 0.15 in the case of $j=2$, the approximation gives only an error of about 15% at most. Actually the error is much smaller than 15% in the case of $j=2$. In the other terms, $\exp(i2K\Delta)$ is approximated by $1 + i2K\Delta$. These approximations become poor when j becomes large. However, the case of smaller j ($j \lesssim 4$) seems to be of interest. Therefore, we take these approximations. The magnitudes of the r th intervalley minigaps are given by the absolute values of M_r .

At low concentrations ($N_{\text{eff}} \lesssim 2$), the imaginary part of S_0 is much larger than its real part, and¹⁸

$$S_0 \approx -i 1.4 \times 10^{-2} N_{\text{eff}}, \quad (18)$$

or

$$-\frac{\hbar^2 L}{2m} S_0 = i \frac{1.4}{\pi} \times 10^{-13} N_{\text{eff}} \quad (19)$$

in units of meV cm², with

$$N_{\text{eff}} = (N_{\text{inv}} + \gamma N_{\text{depl}}) / 10^{12} \text{ cm}^{-2}, \quad (20)$$

where N_{inv} and N_{depl} are areal concentrations in the inversion layer and depletion layer, respectively; γ is very close to 3. The density dependence of S_0 is shown in Fig. 3. The real part of S_2 is very small: In the range of $0 < N_{\text{eff}} < 10$, the imaginary part of S_2 is 15 times or more as large as its real part. Therefore, the real part of S_2 can be neglected,

$$S_2 \frac{\hbar^2 L}{2m} \approx i 10 N_{\text{eff}} \quad (21)$$

in units of meV.

The magnitude of the r th intervalley minigap is evaluated as

$$E_r = \left[2.8 \times 10^{-2} \Xi e_{xy} B_r / (1 \text{ meV}) + \sin 2\phi \left(1.4 \times 10^{-13} \frac{k_n^2}{\pi} B_r + 23 \frac{\theta}{\alpha} + O(\theta^2) \right) \right] \frac{\sin(r\pi\theta\alpha)}{r\pi\theta\alpha} e^{-(r/j)^2 w^2 N_{\text{eff}}} \quad (22)$$

in units of meV, for $N_{\text{eff}} \lesssim 2$ where

$$B_r = \begin{cases} 1 & (r=0), \\ 0.15(j/2r) & (r \neq 0), \end{cases} \quad (23)$$

and $\sin(x)/x$ is defined to be 1 at $x=0$. Here and in the following, k_n is in units of cm⁻¹. An expression is slightly changed for higher concentrations ($N_{\text{eff}} \gtrsim 2$), because the real part of S_0 becomes larger than its imaginary part, as shown in Fig. 3. For example, the formula for E_0 is changed as follows;

$$E_0 \approx \begin{cases} 23(\theta/\alpha) \sin 2\phi N_{\text{eff}} \text{ meV} & (N_{\text{eff}} < 2) \\ 16(\theta/\alpha) \sin 2\phi N_{\text{eff}} \text{ meV} & (N_{\text{eff}} > 8) \end{cases} \quad (24)$$

for stress-free samples and $k_n = 0$. The coefficient becomes smaller for higher N_{eff} .

In flat planes ($j=0$), only E_0 is finite and its magnitude is¹⁸

$$E_0 = \left[2.8 \times 10^{-2} \Xi e_{xy} / (1 \text{ meV}) + \sin 2\phi \left(1.4 \times 10^{-13} \frac{k_n^2}{\pi} + 10\theta^2 \right) N_{\text{eff}} \right]. \quad (25)$$

in units of meV.

Intravalley minigaps open at $k_t = (0.15/2 \pm r/j)Q$ for (+) valleys, and at $k_t = (-0.15/2 \pm r/j)Q$ for (-) valleys ($r \geq 1$). Their magnitudes are calcula-

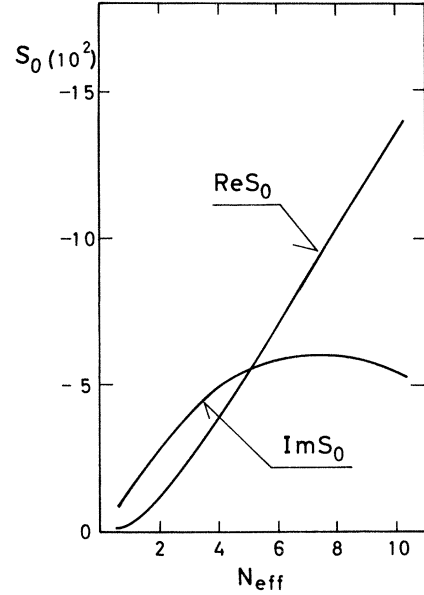


FIG. 3. Overlap integral S_0 as a function of N_{eff} , where $N_{\text{eff}} = (N_{\text{inv}} + 3N_{\text{depl}}) / 10^{12} \text{ cm}^{-2}$ is an effective charge concentration in an inversion layer.

ted as

$$A_r = 2 |F b_r + T C_r(0)| \approx [(0.23j/r)^2 + (83)^2(\theta/\alpha - 2\theta^2)^2 N_{\text{eff}}^{-2/3}]^{1/2} \times \frac{\sin(r\pi\theta\alpha)}{r\pi\theta\alpha} e^{-(r/j)^2 w^2 N_{\text{eff}}}, \quad (26)$$

again in units of meV, where use is made of

$$F = \frac{4\pi e^2}{k_s} \left(\frac{1}{\gamma} N_{\text{inv}} + N_{\text{depl}} \right). \quad (27)$$

In flat planes ($j=0$), intravalley minigaps vanish. Intravalley minigaps have a weak θ dependence as long as θ is small ($|r|\pi\theta\alpha \ll 1$), and their magnitudes are of the same order as the intervalley minigaps. When there exists a staircase structure, many properties are modified such as an image potential, polarization of an insulator, and a semiconductor and the electron distribution.²⁵ If such effects are included, the coefficient 0.23 in Eq. (26) will have a small change.

V. DISCUSSION

So far, the lowest four minigaps have been observed in the (11 \bar{n}) planes.³ Their positions can be well explained by a model where step heights are of a half-lattice constant ($a/2$). This model is the most probable one from a physical point of

view. The following are very physical assumptions: (i) an interface should be macroscopically flat and be the (lmn) plane, and (ii) step heights should be as short as possible, because shorter step heights give flatter interfaces. Because an Si lattice is an fcc one, it is the most probable that almost all step heights are of half a lattice constant; special preparations should be required to obtain step heights with $a/4$. In fact, normally treated free surfaces have step height with half a lattice constant.²⁰

In this physical model, the lowest minigap is E_0 . The next ones are $E_1, A_1, E_{-1}, E_2, A_2, E_{-2}, E_3$, and so on in this order. Our result can explain well the observed magnitude of the lowest one, E_0 . Sesselmann and Kotthaus¹¹ fitted their data in a form predicted by a flat interface model. An agreement between experiment and theory is not so good in a flat interface model. Figure 4 shows a replotting of their data, and

$$E_0 = \left(0.9 \times 10^{-13} \frac{k_\eta^2}{\pi} + 7.7\theta\right) N_{\text{inv}} \text{ meV} \quad (28)$$

is obtained, where k_η is in units of cm^{-1} . Kamgar, Sturge, and Tsui obtained¹²

$$E_0 = (1.4 \times 10^{-13} N_{\text{inv}} + 7.5\theta) N_{\text{inv}} \text{ meV}. \quad (29)$$

In Eqs. (28) and (29), N_{inv} is in units of 10^{12} cm^{-2} . In order to explain their data, we have to take $\alpha = \sin(\theta + \lambda)/\cos\lambda \approx \tan\lambda \approx 3.1$. This is not unreasonable, because the geometrical consideration shows that $\tan\lambda$ is about $\sqrt{2}$ for $(11n)$ planes.

The interface location $\Delta(\xi, \eta)$ discussed here should be considered to be an effective one. The approximation used here can be expressed in a

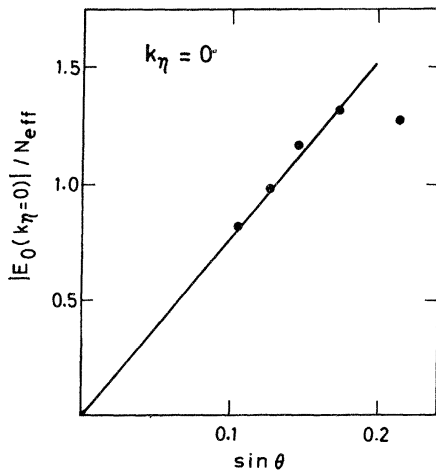


FIG. 4. Experimental data for the lowest minigap E_0 at $k_\eta = 0$ by Sesselmann and Kotthaus (Ref. 11). The data can be fitted by $7.7 \sin\theta N_{\text{eff}}$ meV.

simpler form than the wave function of the ground subband is assumed to be:

$$\exp[i(\pm K\theta + k_\xi)\xi + ik_\eta\eta]\phi[\xi - \Delta(\xi, \eta)]. \quad (30)$$

This means that Δ shows how the wave function is distorted by a staircase. Our model includes a parameter α or λ , which expresses the structure of steps. The step length ($\frac{1}{2}\alpha a$ in Fig. 1) is about 3.5 \AA , if a geometrical plane is taken. However, it is very short compared to the width of inversion layers (about 30 \AA), and it is very difficult for electrons to follow such a rapid distortion of interfaces. Our analysis shows that $\frac{1}{2}\alpha a$ is about 8.5 \AA , and this scale is a very reasonable one for electrons to follow a distortion. One can conclude that Δ discussed here is an effective location of interfaces. One can also explain by this discussion that α is nearly independent of θ . It should be noted that the above discussion is only valid as far as $\alpha\theta$ is much less than $\frac{1}{2}$.

Kamgar *et al.*¹² also reported the magnitude of the second minigap; $E_1 = (2.75 \pm 0.3) \text{ meV}$ at $N_{\text{inv}} = 3.1 \times 10^{12} \text{ cm}^{-2}$ and $\theta = 3.3 \times 10^{-2}$ (1.9°). This is a little larger than a theoretical one ($\approx 1 \text{ meV}$). Our theory gives the magnitudes of E_r at $k_\eta = 0$ as

$$E_r = 23 \left(\frac{\theta}{\alpha}\right) \sin 2\phi \frac{\sin(r\pi\theta\alpha)}{r\pi\theta\alpha} e^{-(r/s)^2 W^2} N_{\text{eff}} \quad (31)$$

with E_r in units of meV. It is very interesting to check this dependence in higher intervalley minigaps. If W is determined experimentally, it gives information about the staircase structures. The factor W is a kind of Debye-Waller factor which specifies the disorder of the staircase structures. It is also interesting to check Eq. (26) for intervalley minigaps.

If no disorder exists at the interfaces, the dependence of E_r and A_r on θ is not a smooth function because of the commensurability. However, a disorder makes the θ dependence smooth in actual samples.

Intervalley minigaps have a $\sin 2\phi$ dependence; they should vanish in $(01n)$ planes. Current experimental data for E_0 show a sample dependence on $(01n)$ planes.^{5,13} In some samples, rather large minigaps are observed, while very small ones are observed in the other samples. A built-in shear strain is one possible explanation for this sample dependence. Strain contribution is estimated as $2.8 \times 10^{-2} \Xi e_{xy} N_{\text{eff}}$ for E_0 . Since Ξ is several eV, shear strain as large as $2 \sim 5 \times 10^{-3}$ is necessary. This magnitude of strain is not unreasonable. On the other hand, it is of interest to investigate the shear strain dependence of the intervalley minigaps. The shear strain e_{xy} can be obtained by a uniaxial stress along $[110]$ or $[1\bar{1}0]$. A uniaxial compression along $[110]$ has the same effect as a

uniaxial tension along $[1\bar{1}0]$, but a different effect to a uniaxial compression along $[1\bar{1}0]$ or to a uniaxial tension along $[110]$. The effect is large on the lowest intervalley minigap, but smaller on the higher ones.

The so-called Γ coupling is neglected here. When this coupling is included, the intervalley minigap at $k_x = 2\pi\theta/a$ in Fig. 2 is slightly modified and becomes a little larger. This contribution includes a term independent of θ . Therefore, the Γ coupling becomes a major contribution to the minigap at $k_x = 2\pi\theta/a$ for very small θ . This contribution does not change, even if the staircase structure is taken into account.

Intravalley minigaps do not have an explicit ϕ dependence. If the staircase structure depends on ϕ , then the intravalley minigaps also depend on ϕ ; an implicit ϕ dependence is possible. For a very small θ , the period is very long, $(ja/4\theta)$. If this length is longer than the mean free path of electrons, electrons cannot "feel" the periodic potential. Therefore, our result cannot be applied to the case with very small θ . Neither can our result be applied to the case where $\hbar^2 j^2 Q^2 / 2m_i$ is less than A_r , because the first-order treatment breaks down then.

Ando discussed the dc conductivity in tilted planes, and claimed that there should be significant intervalley scatterings in order to explain the observed line shape of dc conductivity.²⁶ It is very

reasonable to conclude from Eq. (6) in the present paper that the surface roughness contributes to intervalley scattering as much as intravalley ones.

VI. SUMMARY

A one-dimensional staircase model is investigated. It is a straightforward idea that a periodic staircase gives rise to intravalley minigaps. The present investigation shows that a staircase has also a large effect on intervalley minigaps. Our analysis of experimental data shows that step heights are of half a lattice constant, and that the period is $a/(2\sin\theta)$ where a is the lattice constant. The positions of minigaps given by this staircase model are exactly the same as the valley projection model by Sham *et al.*⁶

The magnitudes of minigaps are given by Eqs. (22) and (26). Our theory can explain the magnitude of the lowest minigap measured by Sesselmann and Kotthaus,¹¹ and Kamgar *et al.*¹² A possible determination of a precise staircase structure by comparing the present theoretical results to the experimental result is suggested.

ACKNOWLEDGMENTS

The author thanks Professor L.J. Sham for useful discussion. This work is supported by the National Science Foundation, Contract No. NSF DMR 77-09595.

*Present address: The Institute for Solid State Physics, University of Tokyo, Minato-ku, Tokyo 106, Japan.

¹T. Ando, Surf. Sci. **98**, 327 (1980).

²T. Cole, A. A. Lakhani, and P. J. Stiles, Phys. Rev. Lett. **38**, 722 (1977).

³D. C. Tsui, M. D. Sturge, A. Kamgar, and S. J. Allen, Jr., Phys. Rev. Lett. **40**, 1667 (1978).

⁴A. A. Lakhani, T. Cole, and P. J. Stiles, Surf. Sci. **73**, 223 (1978).

⁵K. Kusuda and S. Kawaji (private communication).

⁶L. J. Sham, S. J. Allen, Jr., A. Kamgar, and D. C. Tsui, Phys. Rev. Lett. **40**, 472 (1978).

⁷D. C. Tsui, S. J. Allen, Jr., R. A. Logan, A. Kamgar, and S. N. Coppersmith, Surf. Sci. **73**, 419 (1978).

⁸D. C. Tsui and E. Gornik, Appl. Phys. Lett. **32**, 365 (1978).

⁹T. Cole, J. P. Kotthaus, T. N. Theis, and P. J. Stiles, Surf. Sci. **73**, 238 (1978).

¹⁰W. Sesselmann, T. Cole, J. P. Kotthaus, R. Keller, H. Gesch, I. Eisele, G. Dorda, and P. Goy, in *Physics of Semiconductors, 1978*, edited by B. L. H. Wilson (Institute of Physics, Bristol, 1979), p. 1343.

¹¹W. Sesselmann and J. P. Kotthaus, Solid State Commun. **31**, 193 (1979).

¹²A. Kamgar, M. D. Sturge, and D. C. Tsui, Phys. Rev.

B **22**, 841 (1980).

¹³H. Okamoto, K. Muro, S. Narita, and S. Kawaji, Surf. Sci. **98**, 505 (1980).

¹⁴V. A. Volkov and V. B. Sandomirskii, Pis'ma Zh. Eksp. Teor. Fiz. **27**, 688 (1978) [JETP—Lett. **27**, 651 (1978)].

¹⁵L. J. Sham, in *Physics of Semiconductors, 1978*, edited by B. L. H. Wilson (Institute of Physics, Bristol, 1979), p. 1339.

¹⁶F. J. Ohkawa, J. Phys. Soc. Jpn. **45**, 1427 (1978).

¹⁷F. J. Ohkawa, J. Phys. Soc. Jpn. **46**, 855 (1979).

¹⁸F. J. Ohkawa, Surf. Sci. **98**, 350 (1980).

¹⁹M. Hentzler, Surf. Sci. **73**, 240 (1978).

²⁰R. Kaplan, Surf. Sci. **93**, 145 (1980).

²¹J. C. Hensel, H. Hasegawa, and M. Nakayama, Phys. Rev. **138**, A225 (1965).

²²F. J. Ohkawa and Y. Uemura, J. Phys. Soc. Jpn. **43**, 907 (1977); **43**, 917 (1977); **43**, 925 (1977).

²³L. J. Sham and M. Nakayama, Phys. Rev. B **20**, 734 (1979).

²⁴Y. Matsumoto and Y. Uemura, Proceedings of the International Conference on Solid Surfaces, Kyoto, 1974 [Jpn. J. Appl. Phys. (1974) Suppl. 2, Pt. 2, p. 367].

²⁵T. Ando, J. Phys. Soc. Jpn. **43**, 1616 (1977).

²⁶T. Ando, J. Phys. Soc. Jpn. **47**, 1595 (1979).